# Finite-size and asymptotic behaviors of the gyration radius of knotted cylindrical self-avoiding polygons

Miyuki K. Shimamura
*Department of Applied Physics, Graduate School of Engineering, University of Tokyo, 7-3-1 Hongo, Bunkyo-ku, Tokyo 113-8656, Japan*

Tetsuo Deguchi
*Department of Physics, Faculty of Science, Ochanomizu University, 2-1-1 Ohtsuka, Bunkyo-ku, Tokyo 112-8610, Japan*
(Received 7 February 2002; published 20 May 2002)

Several nontrivial properties are shown for the mean-square radius of gyration $R_K^2$ of ring polymers with a fixed knot type $K$. Through computer simulation, we discuss both finite size and asymptotic behaviors of the gyration radius under the topological constraint for self-avoiding polygons consisting of $N$ cylindrical segments with radius $r$. We find that the average size of ring polymers with the knot $K$ can be much larger than that of no topological constraint. The effective expansion due to the topological constraint depends strongly on the parameter $r$ that is related to the excluded volume. The topological expansion is particularly significant for the small $r$ case, where the simulation result is associated with that of random polygons with the knot $K$.

DOI: 10.1103/PhysRevE.65.051802 PACS number(s): 36.20.−r, 05.40.Fb, 61.41.+e

## I. INTRODUCTION

A ring polymer is one of the simplest systems that exhibit the effect of topological entanglement. The topological state of a ring polymer is given by a knot, and it is fixed after the ring polymer is formed. The entropy of the ring polymer with the fixed knot is much smaller than that of no topological constraint. Thus, there should be several nontrivial properties in statistical mechanics of ring polymers with a fixed topology. Furthermore, some dynamical or thermodynamical properties of ring polymers under topological constraints could also be nontrivial. In fact, various computer simulations of ring polymers with fixed topology were performed by several groups [1–12]. However, there are still many unsolved problems related to the topological effect, such as the average size of a knotted ring polymer in solution.

In this paper, we discuss how the excluded volume controls the topological effect on the average size of ring polymers in good solution. As a model of ring polymers we employ a model of self-avoiding polygons (SAPs) consisting of cylindrical segments with radius $r$. First, we numerically construct a large number of $N$-noded cylindrical SAPs with radius $r$, and evaluate the mean-square radius of gyration $R^2$ of the SAPs under no topological constraint. Then, through some knot invariants we select such SAPs that should have a fixed knot type $K$, and then calculate the mean-square radius of gyration $R_K^2$ of the SAPs with the knot $K$ [13–15]. Comparing the mean square $R_K^2$ with $R^2$, we show various topological effects in the average size of ring polymers under the topological constraint. By changing the cylinder radius $r$, we modify the excluded volume effect. Thus, we can investigate the topological effect systematically through the simulation of cylindrical SAPs for various values of cylinder radius $r$.

Let us consider the two cases when the radius $r$ is very large or very small. When the radius $r$ is very large, the simulation should be related to that of the self-avoiding polygons on the lattice [11,15]. On the other hand, when the radius $r$ is very small, it is related to random polygons with a fixed topology, as we shall see explicitly through the data. In fact, there is quite an interesting suggestion [16–18] that under a topological constraint the average size of ring polymers with no excluded volume should be similar to that of ring polymers with the excluded volume, since nontrivial entropic repulsion should be derived from the topological constraint. According to the suggestion, the average size of random polygons with the trivial knot should be given by $N^{\nu_{\mathrm{SAW}}}$ with respect to the number $N$ of polygonal nodes, where $\nu_{\mathrm{SAW}}$ is the exponent of self-avoiding walks (SAW). Thus, the small $r$ case of the simulation in the paper should be important also in the study of the topological effect on random polygons.

We now discuss an asymptotic behavior of the average size of $N$-noded cylindrical SAPs with a fixed knot $K$, where we send the number $N$ of polygonal nodes to infinity. Let us assume that when $N$ is very large, the average size of ring polymers with or without a topological constraint should be approximately given by some power of $N$ with correction terms. For instance, the mean-square radius of gyration $R^2$ of cylindrical SAPs under no topological constraint can be expressed by the following: $R^2 = AN^{2\nu}[1 + BN^{-\Delta} + O(1/N)]$. Applying the asymptotic expansion to the data of $R_K^2$ versus $N$, we evaluate the best estimates of the exponent $\nu_K$. Then we find that when $N$ is large enough, the asymptotic expansion should be valid both for $R^2$ and $R_K^2$ of the cylindrical SAPs with the knot $K$. Furthermore, we also find that the value of the exponent $\nu_K$ should be consistent with that of SAW: $\nu_K = \nu_{\mathrm{SAW}}$ with respect to errors.

The outline of the paper is given in the following. In Sec. II we explain SAPs consisting of cylinderical segments. We also discuss the effective exponent of the mean-square radius of gyration under no topological constraint $R^2$. In Sec. III, we discuss various nontrivial finite-size properties of the mean-square radius of gyration $R_K^2$ for cylindrical SAPs with a given knot type $K$. When the ratio $R_K^2/R^2$ is larger than 1,

 

then it shows the effective expansion due to the topological constraint. Through the simulation, we find that the topological effect is important particularly in the small $r$ case for cylindrical SAPs. Furthermore, the effective topological expansion is controlled by the parameter $r$. In Sec. IV, we discuss the asymptotic expansion of the ratio $R_K^2/R^2$ with respect to the number $N$. Through the numerical analysis, we conclude that the exponent $\nu_K$ should be consistent with that of SAW. Finally, in Sec. V, we graphically explain the effective expansion of the cylindrical SAPs under the topological constraint, through the graphs in the $N$-$r$ plane.

## II. CYLINDRICAL SELF-AVOIDING POLYGONS

### A. Cylindrical ring-dimerization algorithm and random knots

Let us introduce a model of ring polymers in good solution. We consider self-avoiding polygons consisting of $N$ rigid impenetrable cylinders of unit length and diameter $r$: there is no overlap allowed for any nonadjacent pairs of cylindrical segments, while next-neighboring cylinders may overlap each other. We call them cylindrical self-avoiding polygons or cylindrical SAPs, for short. The cylinder radius $r$ can be related to the stiffness of some stiff polymers such as DNAs [6,14].

In the simulations of the paper, we have constructed a large number of cylindrical SAPs by the cylindrical ring-dimerization method [13]. The method is based on the algorithm of ring dimerization [4], and very useful for generating long self-avoiding polygons (for details, see Ref. [14]). Here we note that another algorithm is discussed in Ref. [6] for the model of cylindrical SAPs, where self-avoiding polygons of impenetrable cylinders with $N<100$ are constructed in association with knotted DNAs [19,20].

In the cylindrical ring-dimerization method, a statistical weight is given to any self-avoiding polygon successfully concatenated. Thus, when we evaluate some quantity, we take the weighted average of it with respect to the statistical weight. Some details on the statistical weight of successful concatenation is given in Ref. [14]. Hereafter in the paper, however, we do not express the statistical weight, for simplicity.

Let us describe the processes of our numerical experiments. First, we construct $M$ samples of cylindrical SAPs with $N$ nodes by the cylindrical ring-dimerization method. We put $M=10^4$. Here we note that various knot types are included in the $M$ random samples. Second, we make knot diagrams for the three-dimensional configurations of cylindrical SAPs, by projecting them onto a plane. Then, we calculate two knot invariants $\Delta_K(-1)$ and $v_2(K)$ for the knot diagrams. Third, we select only such polygons that have the same set of values of the two knot invariants, and then evaluate physical quantities such as mean-squared gyration radius for the selected cylindrical SAPs.

The symbol $\Delta_K(-1)$ denotes the determinant of a knot $K$, which is given by the Alexander polynomial $\Delta(t)$ evaluated at $t=-1$. The symbol $v_2(K)$ is the Vassiliev invariant of the second degree [21,22]. The two knot invariants are practically useful for computer simulation of random polygons with a large number of polygonal nodes. In fact, it has been demonstrated in Ref. [21] that the Vassiliev invariant $v_2(K)$ can be calculated not only in polynomial time but also without using large memory area.

### B. Characteristic length of random knotting $N_c(r)$

For a given knot $K$, we consider the probability $P_K(N,r)$ that the topology of an $N$-noded self-avoiding polygon with cylinder radius $r$ is given by the knot type $K$. We call it the knotting probability of the knot $K$. Let us assume that we have $M_K$ self-avoiding polygons with a given knot type $K$ among $M$ samples of cylindrical SAPs with radius $r$. Then, we evaluate the knotting probability $P_K(N,r)$ by $P_K(N,r)=M_K/M$.

For the trivial knot, the knotting probability $P_{triv}(N,r)$ for the cylindrical SAPs is given by

$$P_{triv}(N,r)=C_{triv}\exp[-N/N_c(r)]. \tag{1}$$

Here the estimate of the constant $C_{triv}$ is close to 1.0 [13]. We call $N_c(r)$ the characteristic length of random knotting. It is also shown in Ref. [13] that $N_c(r)$ can be approximated by an exponential function of $r$,

$$N_c=N_c(0)\exp(\gamma r). \tag{2}$$

The best estimates of the two parameters $N_c(0)$ and $\gamma$ are given by $N_c(0)=292\pm5$ and $\gamma=43.5\pm0.6$ [13].

For several knots, it is shown [14] that the knotting probability $P_K(N,r)$ of a knot $K$ is given by

$$P_K(N,r)=C_K\left(\frac{N}{N_K(r)}\right)^{m(K)}\exp[-N/N_K(r)]. \tag{3}$$

It is numerically suggested in Ref. [14] that $N_K(r)$ should be independent of $K$: $N_K(r)\approx N_c(r)$, and also that the constant $C_K$ should be independent of the cylinder radius $r$.

We note that the formula given in Eq. (3) has been shown for some off-lattice models in the case of the trivial knot [5,8] and some nontrivial knots [9,10]. Furthermore, it has also been shown for the lattice models with some knots [11].

### C. Mean-squared gyration radius with a topological constraint

The mean-square radius of gyration $R^2$ of a self-avoiding polygon is defined by

$$R^2=\frac{1}{2N^2}\sum_{n,m=1}^{N}\langle(\vec{R}_n-\vec{R}_m)^2\rangle. \tag{4}$$

Here $\vec{R}_n$ is the position vector of the $n$th segment (or the $n$th node) and $\langle\cdot\rangle$ denotes the ensemble average, which is taken over all possible configurations of the self-avoiding polygon.

Suppose that we have $M$ self-avoiding polygons. Then, we evaluate the mean-square radius of gyration $R^2$ by the

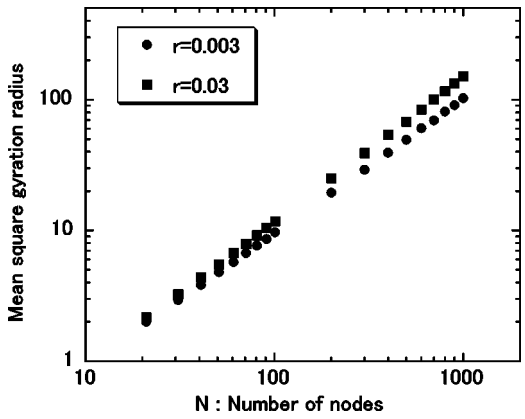


FIG. 1. Double-logarithmic plots of the mean-square radius of gyration under no topological constraint $R^2$ for cylindrical SAPs versus the number $N$ of polygonal nodes for radius $r=0.003$ and 0.03 depicted by closed circles and squares, respectively.

sum: $R^2=\Sigma_{i=1}^{M}R_i^2/M$, where $R_i^2$ denotes the gyration radius of the $i$th SAPs in the given $M$ SAPs.

Let us define the mean-square radius of gyration $R_K^2$ for such self-avoiding polygons that have a given knot type $K$,

$$R_K^2=\frac{1}{M_K}\sum_{i=1}^{M_K}R_{K,i}^2, \tag{5}$$

where $R_{K,i}^2$ denotes the gyration radius of the $i$th self-avoiding polygon that has the knot type $K$. In terms of $R_K^2$, $R^2$ is given by $R^2=\Sigma_K R_K^2 M_K/M$.

In Fig. 1, the estimates of the mean-square radius of gyration $R^2$ are plotted against the number $N$ of nodes in a double-logarithmic scale, for the cylindrical SAPs with $r=0.003$ and $r=0.03$. We may confirm the standard asymptotic behaviors of the mean-squared gyration radius $R^2$ in Fig. 1. Here we remark on an effective exponent $\nu_{\rm eff}$, which is defined through the power-law approximation, $R\sim N^{\nu_{\rm eff}}$. It is shown in Ref. [23] that the estimate of the effective exponent $\nu_{\rm eff}$ for the cylindrical SAPs with radius $r$ is consistent with that of the cylindrical SAWs with radius $r$. However, both for the cylindrical SAWs and SAPs, the estimates of $\nu_{\rm eff}$ are smaller than $\nu_{\rm SAW}$, partially because the range of $N$ is limited upto 1000 in the data of Fig. 1. Thus, we have $\nu_{\rm eff}=0.514$ for $r=0.003$ and $\nu_{\rm eff}=0.556$ for $r=0.03$ (see also Fig. 7.3 of Ref. [23]).

## III. FINITE-SIZE BEHAVIORS OF $R_K^2$ FOR SOME KNOTS

Let us discuss simulation results on the mean-square radius of gyration $R_K^2$ for the cylindrical SAPs with a knot $K$ and of radius $r$. For two prime knots (the trivial and trefoil knots) and a composite knot (the double-trefoil knot, $3_1\sharp 3_1$), we have investigated the mean-squared gyration radius $R_K^2$ under the topological constraint in the range of the number $N$ satisfying $21\leqslant N\leqslant 1001$, and for 14 different values of cylinder radius $r$.

The gyration radius $R_K^2$ can approximately be given by some power of $N$. In Fig. 2, double-logarithmic plots of $R_K^2$ versus $N$ are given for the trivial and trefoil knots, with two values of cylinder radius: $r=0.003$ and 0.03. We see that all the double-logarithmic plots of Fig. 2 fit to some straight lines. We note that for other values of cylinder radius $r$, several double-logarithmic plots of $R_K^2$ versus $N$ are explicitly shown in Ref. [23].

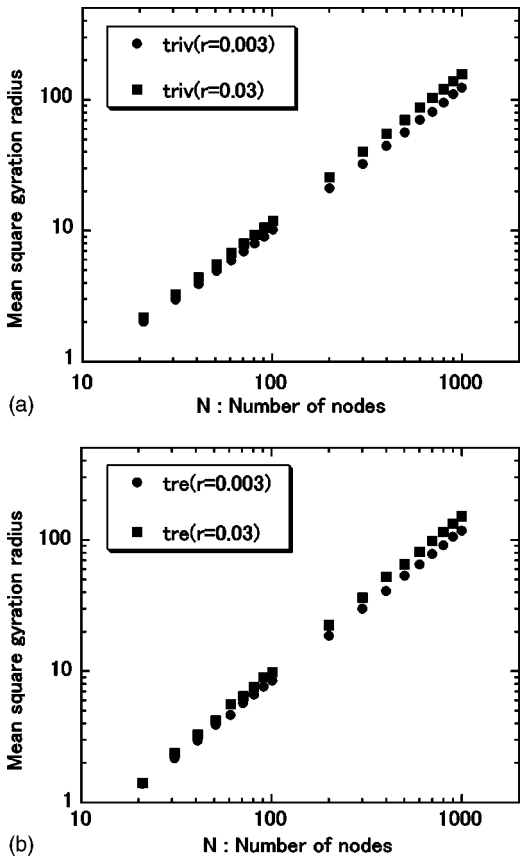


FIG. 2. Double-logarithmic plot of $R_K^2$ versus $N$ with $r=0.003$ and 0.03 shown by closed circles and squares, respectively: (a) for the trivial knot; (b) for the trefoil knot.

With the number $N$ fixed, $R_K^2$ should increase with respect to the radius $r$ for any knot. Both for the trivial knot [Fig. 2(a)] and the trefoil knot [Fig. 2(b)], closed squares for $r=0.03$ are located higher in the vertical direction than closed circles for $r=0.003$, through the whole range of $N$.

### A. Ratio $R_K^2/R^2$ and the effective expansion under the topological constraint

Let us now consider the ratio of $R_K^2$ to $R^2$ for a given knot $K$. If the ratio is larger (smaller) than 1.0, then the average size of SAPs with the knot $K$ is relatively larger (smaller) than that of no topological constraint. We say that the SAPs with the knot $K$ is effectively more (less) expanded. In Fig. 3, the ratio $R_K^2/R^2$ versus the number $N$ is plotted in a double-logarithmic scale for the trivial and trefoil knots. Here, we have depicted only the case of $r=0.003$ among many sets of the cylindrical SAPs with 14 different values of cylindrical radius.

For the trivial knot, we see in Fig. 3 that the ratio $R_{triv}^2/R^2$ is greater than 1.0 when $N>50$. Thus, the average size of the

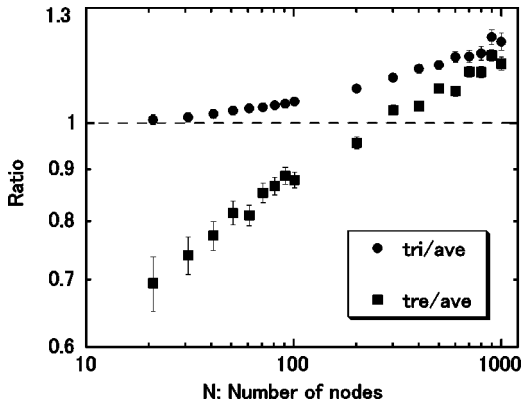


FIG. 3. Double-logarithmic plots of the ratio $R_K^2/R^2$ versus $N$ for cylindrical SAPs with $r=0.003$. $R_{triv}^2/R^2$ and $R_{tre}^2/R^2$ are shown by closed circles and squares, respectively.

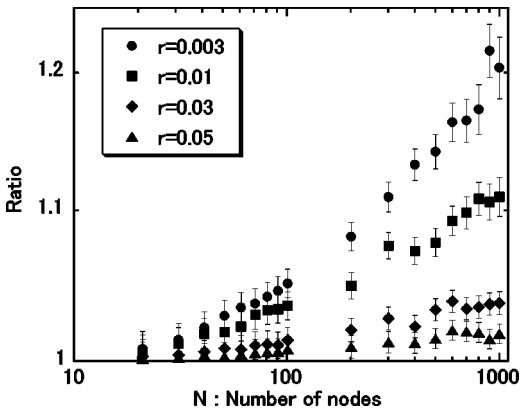


FIG. 4. Double-logarithmic plots of the ratio $R_{triv}^2/R^2$ versus $N$ for $r=0.003$, 0.01, 0.03, and 0.05 shown by closed circles, squares, diamonds and triangles, respectively.

ring polymers with the trivial knot enlarges under the topological constraint. It gives a typical example of effective expansion.

In Fig. 3, the graph of the trivial knot is convex downwards: the ratio $R_{triv}^2/R^2$ is almost constant with respect to $N$ for small $N$ such as $N<100$; for $N>300$ the ratio $R_{triv}^2/R^2$ increases with respect to $N$ with a larger gradient, and the graph can be approximated by a power law such as $R_{triv}^2/R^2 \propto N^{2\,\Delta\nu_{\rm eff}^{triv}}$. Here the symbol $\Delta\nu_{\rm eff}^{triv}$ denotes the effective exponent for the trivial knot. We note that the characteristic length $N_c(r)$ is approximately given by 300 for $r=0.003$. Thus, we may say that the power law behavior is valid for $N>N_c(r)$.

For the trefoil knot, the graph can be approximated by a power of $N$ such as $R_{tre}^2/R^2 \propto N^{2\,\Delta\nu_{\rm eff}^{tre}}$ through the range of $100 \leqslant N \leqslant 1001$. Here the symbol $\Delta\nu_{\rm eff}^{tre}$ denotes the effective exponent of the trefoil knot. In Fig. 3, we find that when $N<100$ the ratio $R_{tre}^2/R^2$ is smaller than 1.0, while it is larger than 1.0 when $N>300$. Thus, when $N$ is small, the topological constraint of the trefoil knot gives effective shrinking to ring polymers, while it does not when $N$ is large. For a nontrivial knot $K$, we expect that the ratio $R_K^2/R^2$ is less than 1.0 when $N$ is small, while it can be larger than 1.0 when $N$ is large.

The properties of the ratio $R_K^2/R^2$ discussed in the three preceding paragraphs are consistent with the simulation results of Gaussian random polygons [24]. We have found for the random polygons that the double-logarithmic graph of $R_K^2/R^2$ versus $N$ is given by a downward convex curve for the trivial knot, while it is given by a straight line for the trefoil knot and also for other several nontrivial knots; for the nontrivial knots investigated, the ratio $R_K^2/R^2$ is given by some power of $N$ such as $N^{2\,\Delta\nu_{\rm eff}^{K}}$. Thus, there are indeed many important properties valid both for the simulation of the Gaussian random polygons and that of the cylindrical SAPs with a small radius such as $r=0.003$.

The observations derived from Fig. 3 should be valid particularly for finite-size systems. Admitting that $N$ is finite, we can only understand that the Gaussian random polygons and the cylindrical SAPs have the similar topological properties in common. If we discuss asymptotic behaviors, SAPs and random polygons should be quite different. However, if we consider such properties that are valid for finite $N$, then they can hold both for SAPs with small excluded volume and random polygons that have no excluded volume.

Let us discuss again the convexity of the graph of the trivial knot, which has been observed in Fig. 3. We consider how the convexity depends on the radius $r$. In Fig. 4, the graphs of the ratio $R_{triv}^2/R^2$ versus $N$ are given in a double-logarithmic scale for four different values of cylinder radius $r$. Then, we see that the graph with $r=0.05$ is less convex than that of $r=0.003$. Thus, the convexity in the graphs of the effective expansion for the trivial knot should be valid only when cylinder radius $r$ is small.

Let us assume that the convexity of the graphs of $R_{triv}^2/R^2$ for the small $r$ case should correspond to a crossover behavior of $R_{triv}^2/R^2$ with respect to $N$. Then, the crossover behavior could be related to that of Gaussian random knots, which has recently been discussed by Grosberg [18] for Gaussian random polygons. We can discuss the convexity of the double-logarithmic graph of $R_{triv}^2/R^2$ versus $N$, taking an analogy with the crossover of the Gaussian random knots. Thus, we call the convexity of the trivial knot in Fig. 3 the crossover, hereafter in the paper.

For the nontrivial knots investigated, we do not see any crossover in the graph of $R_K^2/R^2$ versus $N$. For instance, for the $4_1$ and $3_1 \sharp 3_1$ knots, the slope of the graph near $N \sim N_c(r)$ is straight in the double-logarithmic scale. The crossover at $N \sim N_c(r)$ should be valid only for the trivial knot.

### B. The plateau in the graph of $R_K^2/R^2$ versus $N$ for large $N$

We discuss how the ratio $R_K^2/R^2$ depends on the number $N$, considering both the excluded volume effect and the effective expansion due to the topological constraint. In Fig. 5, the graphs of the ratio $R_K^2/R^2$ versus $N$ for different values of cylinder radius $r$ are shown in linear scales: (a) for the trivial knot; (b) for the trefoil knot.

Let us first consider the large $N$ behaviors of the graphs shown in Fig. 5 for the trivial and trefoil knots. The graphs of

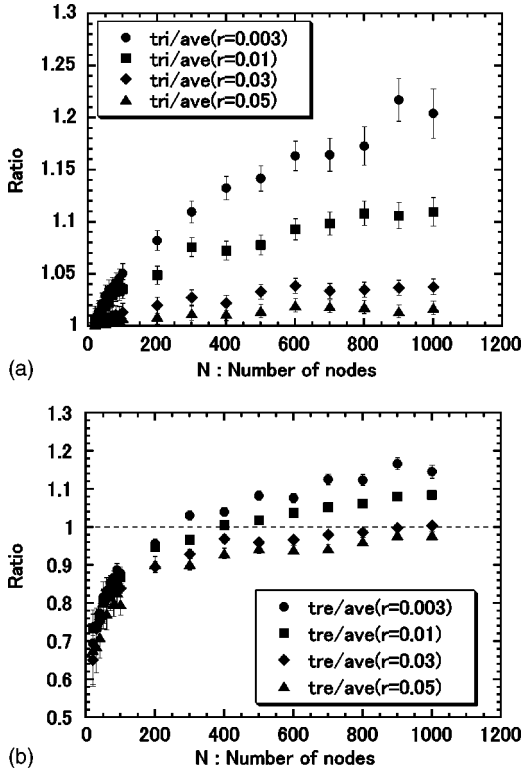


FIG. 5. Graphs of the ratio $R_K^2/R^2$ versus the number $N$ in linear scales for $r=0.003$, 0.01, 0.03, and 0.05 shown by closed circles, squares, diamonds, and triangles, respectively: (a) for the trivial knot and (b) for the trefoil knot. The same data points are shown in both Fig. 4 and Fig. 5(a).

$R_K^2/R^2$ versus $N$ have a common tendency that they become constant with respect to $N$ when $N$ is very large. It is particularly the case for the larger values of cylinder radius $r$ such as $r=0.03$ and 0.05. They approach horizontal lines at some large values of $N$. When $r$ is small such as $r=0.003$, the graph becomes flat only for large $N$, as shown in Fig. 5.

The flatness of the graphs of $R_K^2/R^2$ for large $N$ shows that the exponent $\Delta\nu_K$ for the ratio $R_K^2/R^2$ should be given by zero. Here we have defined $\Delta\nu_K$ by the difference, $\Delta\nu_K = \nu_K - \nu_{\mathrm{SAW}}$. On the other hand, when $N$ is small, the graphs of $R_K^2/R^2$ versus $N$ can be approximated by some power of $N$. Here we recall that in Fig. 3, the power of $N$: $N^{2\,\Delta\nu_{\mathrm{eff}}^{tre}}$ gives a good approximation for the ratio $R_{tre}^2/R^2$ as a function of $N$ through the range of $100 \leqslant N \leqslant 1001$ with $r=0.003$. However, the flatness shows that the power-law approximation does not hold when $N$ is large enough. Thus, the graphs in Fig. 5 reaching their plateau regions for large $N$ also show that the finite-size behavior described by some power of $N$ gradually changes into the asymptotic behavior with $\Delta\nu_K=0$.

Let us discuss other finite-$N$ behaviors of the ratio $R_K^2/R^2$. For the trefoil knot, the ratio $R_{tre}^2/R^2$ is less than 1.0 when $N$ is small; it approaches or becomes larger than 1.0 when $N$ is large enough. When cylinder radius $r$ is small such as $r=0.003$ and $r=0.01$, the ratio $R_{tre}^2/R^2$ is clearly greater than 1.0 when $N$ is large enough. When $r$ is small, there should be a critical value $N_{critical}$ such that $R_{tre}^2/R^2<1.0$ for $N<N_{critical}$, and $R_{tre}^2/R^2>1.0$ for $N>N_{critical}$. Furthermore, we have a conjecture that the critical value $N_{critical}$ should be roughly equal to the characteristic length $N_c(r)$ of random knotting. It seems that the conjecture is consistent with the graphs of Fig. 5(b).

Let us discuss the conjecture on $N_{critical}$, explicitly. In Fig. 5(b), we see that for $r=0.003$, the ratio $R_{tre}^2/R^2$ becomes 1.0 roughly at $N=300$, and also that for $r=0.01$, the ratio $R_{tre}^2/R^2$ is close to 1.0 roughly at $N=400$. The observations are consistent with the estimates of $N_c(r)$ in Ref. [13]: $N_c(r)=(2.72\pm0.06)\times10^2$ for $r=0.0$ and $N_c(r)=(4.72\pm0.14)\times10^2$ for $r=0.01$. Thus, the consistency supports the conjecture on $N_{critical}$.

### C. Decrease of the topological effect under the increase of the excluded volume

The effect of a topological constraint on the gyration radius decreases when the excluded volume increases. There are two examples: the decrease of ratio $R_K^2/R^2$ with respect to cylinder radius $r$ while $N$ being fixed, and the disappearance of the crossover for the trivial knot shown in Figs. 3 and 4.

Let us first discuss how the excluded volume can modify the effective expansion due to the topological constraint. As we clearly see in Fig. 5, the ratio $R_K^2/R^2$ decreases as cylinder radius $r$ increases with $N$ fixed, both for the trivial and trefoil knots. Thus, the effective expansion of SAPs under the topological constraint becomes smaller when the excluded volume becomes larger.

It is quite nontrivial that the effective expansion given by the ratio $R_K^2/R^2$ decreases as cylinder radius $r$ increases. In fact, the value of $R_K^2$ itself increases with respect to $r$, as we have observed in Fig. 2. Furthermore, one might expect that the effective expansion due to a topological constraint should also increase with respect to cylinder radius $r$, simply because the average size of ring polymers with larger excluded volume becomes larger, as observed in Fig. 1. However, it is not the case for the ratio $R_K^2/R^2$.

Let us now discuss the crossover behavior of the trivial knot again, from the viewpoint of the competition between the topological effect and the excluded volume effect. Here we recall that the crossover has been discussed in Sec. III.A with Figs. 3 and 4. Here we regard the crossover as a characteristic behavior derived from the topological constraint of being the trivial knot.

As a working hypothesis, let us assume that the crossover should occur at around the characteristic length $N_c(r)$. Recall that $N_c(r)$ is larger than 1000 for $r=0.03$ and 0.05, as we have estimated: $N_c(r)\approx1200$ for $r=0.03$, and $N_c(r)\approx2600$ for $r=0.05$. If the above hypothesis would be valid, then the graphs for $r=0.03$ and 0.05 should also be convex. In Fig. 4, however, we see no change in the gradient of the graph of $R_{triv}^2/R^2$ versus $N$ for $r=0.03$ or 0.05. The assumed crossover of the trivial knot does not appear for $r=0.03$ or 0.05. We may thus consider that the crossover as a topologi-

cal effect is diminished by the excluded volume effect when $r \geqslant 0.03$.

### D. Characteristic length of random knotting $N_c(r)$ and the effective expansion

In terms of the characteristic length $N_c(r)$, we can explain some properties of the effective expansion of cylindrical SAPs under a topological constraint. Here we recall that the ratio $R_K^2/R^2$ describes the degree of the effective expansion under the topological constraint of a knot $K$.

We first consider the case when the characteristic length $N_c(r)$ is very large. Let us show that the ratio $R_{triv}^2/R^2$ should be close to 1.0 for $N \ll N_c(r)$. First, we recall that the probability $P_{triv}(N)$ of the trivial knot decays exponentially with respect to the number $N$ of polygonal nodes, $P_{triv}(N) = \exp[-N/N_c(r)]$. If $N/N_c(r)$ is very small, the probability $P_{triv}(N)$ is close to 1.0, i.e., almost all SAPs have the trivial knot. Then, the mean-squared gyration radius with no topological constraint $R^2$ should be almost equal to that of the trivial knot $R_{triv}^2$. Consequently, the ratio $R_{triv}^2/R^2$ should be close to 1.0.

When $r \geqslant 0.05$, the characteristic length $N_c(r)$ is larger than 2600. Then, the trivial knot is dominant among the possible knots generated in SAPs with $N < 1000$. Thus, $R_{triv}^2$ should almost agree with $R^2$, which is the mean-squared gyration radius of SAPs under no topological constraint. There is no effective expansion under the topological constraint: the $R_{triv}^2/R^2$ is close to 1.0.

Let us next consider the case when the characteristic length $N_c(r)$ is small or not large. Then we show that the mean-square radius of gyration of SAPs with the trivial knot $R_{triv}^2$ should be larger than that of no topological constraint $R^2$ for $N > N_c(r)$. In fact, various types of knots can appear in a given set of randomly generated SAPs of the cylinder radius $r$, since the probability of the trivial knot $P_{triv}(N)$ is exponentially small for $N > N_c(r)$. We note that the fraction of nontrivial knots is given by $1 - \exp[-N/N_c(r)]$. Thus, it is not certain whether the ratio $R_{triv}^2/R^2$ is close to the value 1.0 or not. However, we may expect that the ratio $R_{triv}^2/R^2$ should be indeed larger than 1.0. Here we consider the following points: when $N > N_c(r)$, the majority of SAPs generated randomly should have much more complex knots than the trivial knot; the mean-square radius of gyration of $N$-noded SAPs with a very complex knot should be much smaller than that of the trivial knot.

The explanation on the effective expansion discussed above is completely consistent with the simulation results, as we have discussed in Sec. III, in particular, through Figs. 3, 4, and 5.

## IV. ASYMPTOTIC BEHAVIORS OF $R_K^2$

### A. The exponent of $R_K^2$

Let us discuss an asymptotic expansion for the mean-square radius of gyration of cylindrical SAPs with a given knot $K$. Here we assume that $R_K^2$ can be expanded in terms of $1/N$ consistently with renormalization group arguments. Then, the large $N$ dependence of $R_K^2$ is given by

$$R_K^2 = A_K N^{2\nu_K}[1 + B_K N^{-\Delta} + O(1/N)]. \tag{6}$$

Here, the exponent $\nu_K$ should be given by that of self-avoiding walks, $\nu_K = \nu_{\mathrm{SAW}}$. In order to analyze the numerical data systematically, however, we have introduced $\nu_K$ as a fitting parameter. Thus, for the ratio $R_K^2/R^2$, we have the following expansion:

$$R_K^2/R^2 = (A_K/A)N^{2\Delta\nu_K}[1 + (B_K - B)N^{-\Delta} + O(1/N)]. \tag{7}$$

Here we have put $\Delta\nu_K$ as a fitting parameter.

TABLE I. Fitting parameters $A_K/A, B_K - B$, and $\Delta\nu_K$ versus cylinder radius $r$: for the trivial knot.

| $r$ | $A_K/A$ | $B_K - B$ | $2\Delta\nu_K$ | $\chi^2$ |
|---|---|---|---|---|
| 0.001 | $1.313 \pm 1.285$ | $-2.587 \pm 4.211$ | $0.003 \pm 0.123$ | 18 |
| 0.002 | $1.235 \pm 1.152$ | $-2.389 \pm 4.117$ | $0.009 \pm 0.116$ | 12 |
| 0.003 | $1.213 \pm 1.065$ | $-2.317 \pm 3.912$ | $0.009 \pm 0.109$ | 3 |
| 0.004 | $1.228 \pm 1.062$ | $-1.982 \pm 3.973$ | $0.003 \pm 0.107$ | 3 |
| 0.005 | $1.170 \pm 0.983$ | $-1.684 \pm 3.985$ | $0.007 \pm 0.104$ | 4 |
| 0.006 | $1.207 \pm 0.921$ | $-2.204 \pm 3.464$ | $0.005 \pm 0.095$ | 4 |
| 0.007 | $1.159 \pm 0.891$ | $-1.633 \pm 3.684$ | $0.005 \pm 0.095$ | 3 |
| 0.01 | $1.106 \pm 0.836$ | $-1.090 \pm 3.809$ | $0.005 \pm 0.092$ | 3 |
| 0.02 | $1.065 \pm 0.686$ | $-0.699 \pm 3.384$ | $0.003 \pm 0.078$ | 1 |
| 0.03 | $1.063 \pm 0.628$ | $-0.518 \pm 3.166$ | $-0.001 \pm 0.071$ | 2 |
| 0.04 | $1.043 \pm 0.590$ | $-0.353 \pm 3.076$ | $-0.001 \pm 0.068$ | 1 |
| 0.05 | $1.010 \pm 0.554$ | $-0.143 \pm 3.039$ | $0.002 \pm 0.066$ | 1 |
| 0.06 | $1.020 \pm 0.551$ | $-0.103 \pm 2.997$ | $-0.001 \pm 0.065$ | 1 |
| 0.07 | $1.013 \pm 0.531$ | $-0.187 \pm 2.898$ | $-0.001 \pm 0.060$ | 1 |

We have analyzed the data for the three different knots: the trivial, trefoil, and $3_1 \sharp 3_1$ knots, applying the expansion (7) to the numerical data of $R_K^2/R^2$ for $N \geqslant 300$. The best estimates of the three parameters are given in Tables I, II, and III for the trivial, trefoil, and $3_1 \sharp 3_1$ knots, respectively.

Let us discuss the best estimates of the difference of the exponents, $\Delta\nu_K$. We see in Tables I, II, and III that all the results of $\Delta\nu_K$ suggest that they should be given by 0.0, with respect to the confidence interval. Let us examine the best estimates more precisely. It is rather clear from Tables I, II, and III that for a given cylinder radius $r$, the best estimates of $\Delta\nu_K$ are independent of the knot type.

There is another evidence supporting that $\Delta\nu_K = 0.0$ for the trivial and trefoil knots. Let us consider the plots of the ratio $R_K^2/R^2$ versus $N$ in Fig. 5 for the trivial and trefoil knots. We recall that the graphs are likely to approach some horizontal lines at some large $N$. The tendency of the graphs becoming flat for large $N$ suggests that $R_K^2$ and $R^2$ should have the same exponent, i.e., $\nu_{\mathrm{SAW}}$.

From the two observations, we conclude that the difference of the exponents is given by 0.0: $\Delta\nu_K = 0.0$ for any value of $r$. There is thus no topological effect on the scaling exponent defined in the asymptotic expansion of $R_K^2$.

TABLE II. Fitting parameters $A_K/A, B_K-B$, and $\Delta\nu_K$ versus cylinder radius $r$: for the trefoil knot.

| $r$ | $A_K/A$ | $B_K-B$ | $2\Delta\nu_K$ | $\chi^2$ |
|---|---|---|---|---|
| 0.001 | 1.286±0.970 | −4.440±2.784 | 0.014±0.096 | 3 |
| 0.002 | 1.215±0.918 | −4.093±2.906 | 0.015±0.095 | 10 |
| 0.003 | 1.202±0.905 | −3.562±3.054 | 0.011±0.094 | 11 |
| 0.004 | 1.176±0.872 | −3.423±3.069 | 0.012±0.093 | 16 |
| 0.005 | 1.176±0.845 | −3.461±2.964 | 0.010±0.090 | 6 |
| 0.006 | 1.113±0.807 | −3.174±3.091 | 0.015±0.090 | 7 |
| 0.007 | 1.084±0.765 | −3.219±2.996 | 0.019±0.088 | 3 |
| 0.01 | 1.103±0.743 | −3.220±2.870 | 0.013±0.084 | 1 |
| 0.02 | 1.068±0.765 | −2.326±3.353 | 0.005±0.088 | 2 |
| 0.03 | 1.058±0.790 | −2.262±3.531 | 0.003±0.091 | 4 |
| 0.04 | 1.003±0.835 | −2.043±4.034 | 0.007±0.101 | 3 |
| 0.05 | 1.007±0.883 | −2.422±4.119 | 0.007±0.107 | 4 |
| 0.06 | 1.029±0.975 | −2.900±4.274 | 0.005±0.116 | 3 |
| 0.07 | 0.998±1.197 | −1.923±5.915 | 0.002±0.146 | 2 |

### B. Amplitude ratio $A_K/A$

Let us now consider the amplitude $A_K$ of the asymptotic expansion (7). In Tables I, II, and III, the best estimates of the ratio $A_K/A$ are larger than 1.0 for the three knots, when $r$ is small. The observation must be important. In fact, if the amplitude ratio $A_K/A$ is larger than 1.0 in the asymptotic expansion (7), then $R_K^2$ is larger than $R^2$ for any large value of $N$.

However, there is a clear evidence for the observation that $A_K/A>1.0$ for some small values of cylinder radius $r$. In fact, the graphs of the ratio $R_K^2/R^2$ versus $N$ are monotonically increasing with respect to $N$, as we see in Figs. 3, 4, and 5. It is clear that the graphs with the smaller values of cylinder radius $r$ are larger than 1.0 when $N$ is large. These observations of Figs. 3, 4, and 5 confirm that $A_K/A>1.0$ when cylinder radius $r$ is small. Thus, we may conclude that the topological constraint gives an effective expansion also to asymptotically large cylindrical SAPs when the radius $r$ is small.

The value of $A_K/A$ decreases with respect to the radius $r$ for the three knots. We see it in Tables I to III, where the best estimates of $A_K/A$ are listed. It is also consistent with the fact that the ratio $R_K^2/R^2$ decreases with respect to $r$, which we have discussed in Sec. III C. However, the decrease of $A_K/A$ is quite nontrivial, since the mean-squared gyration radius $R_K^2$ itself increases with respect to $r$, for the trivial and trefoil knots, as shown in Fig. 2. Here we recall in Fig. 1 that the gyration radius under no topological constraint $R^2$ increases with respect to $r$.

TABLE III. Fitting parameters $A_K/A, B_K-B$, and $\Delta\nu_K$ versus cylinder radius $r$: for the double-trefoil knot $(3_1\sharp 3_1)$.

| $r$ | $A_K/A$ | $B_K-B$ | $2\Delta\nu_K$ | $\chi^2$ |
|---|---|---|---|---|
| 0.001 | 1.269±1.158 | −5.203±3.255 | 0.012±0.116 | 7 |
| 0.002 | 1.224±1.077 | −5.203±3.113 | 0.016±0.112 | 7 |
| 0.003 | 1.158±1.090 | −4.371±3.662 | 0.016±0.118 | 1 |
| 0.004 | 1.149±1.054 | −4.866±3.401 | 0.018±0.116 | 9 |
| 0.005 | 1.137±1.008 | −4.851±3.297 | 0.016±0.112 | 4 |
| 0.006 | 1.096±1.002 | −4.745±3.476 | 0.021±0.115 | 1 |
| 0.007 | 1.061±1.043 | −3.819±4.091 | 0.020±0.122 | 3 |
| 0.01 | 1.076±1.369 | −3.563±5.287 | 0.012±0.159 | 4 |

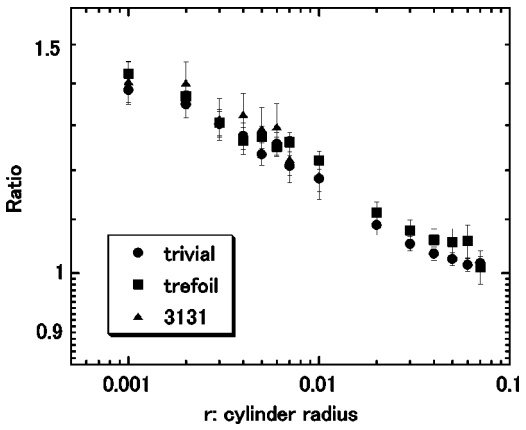


FIG. 6. Double-logarithmic plots of the amplitude ratio $\alpha_K$ versus cylinder radius $r$ for the trivial, trefoil, and double-trefoil $(3_1\sharp 3_1)$ knots shown by closed circles, squares, and triangles, respectively. For the double-trefoil knot, the data points for $0.001 \leqslant r \leqslant 0.01$ are shown.

From the viewpoint of asymptotic behavior, we have shown that the effective expansion derived from the topological repulsion decreases with respect to cylinder radius $r$. We have also discussed that $R_K^2$ is larger than $R^2$ for any large value of $N$, when cylinder radius $r$ is small.

### C. The $r$ dependence of the amplitude ratio

Let us discuss the $r$ dependence of the amplitude ratio $A_K/A$, more quantitatively. For this purpose, we analyze the data of $R_K^2/R^2$ versus $N$ again, assuming $\nu_K=\nu$ in Eq. (7). We evaluate the amplitude ratio $A_K/A$ by the following formula:

$$R_K^2/R^2=\alpha_K[1+\beta_K N^{-\Delta}+O(1/N)]. \tag{8}$$

Here we have replaced with $\alpha_K$ and $\beta_K$, $A_K/A$ and $B_K-B$ in Eq. (7), respectively. Here we have also introduced a technical assumption: $\Delta=\Delta_K=0.5$ in Eq. (7).

We have obtained the numerical estimates of $\alpha_K$, applying the fitting formula (8) to the data of $R_K^2/R^2$ with $N \geqslant 300$ . The estimates of $\alpha_K$ versus $r$ are shown in Fig. 6 in the double-logarithmic scale for the trivial, trefoil, and $3_1\sharp 3_1$ knots. To be precise, the values of $\alpha_K$ are a little larger than those of $A_K/A$ given in Tables I, II, and III.

The estimate of the parameter $\alpha_K$ becomes close to the value 1.0 when cylinder radius $r$ is large enough. Furthermore, it is suggested from Fig. 6 that $\alpha_K$ should be independent of the knot type. In fact, the data points for the trivial, trefoil, and the double-trefoil $(3_1\sharp 3_1)$ knots overlap each other. These two observations are consistent with the simulation result of the self-avoiding polygons on the lattice [7,11].

Interestingly, we see in Fig. 6 that the ratio $\alpha_K$ decreases monotonically with respect to the cylinder radius $r$. For the data with $0.001 \leqslant r \leqslant 0.01$, we find that $\alpha_K$ is roughly approximated by a decreasing function of $r$ such as $\alpha_K = \alpha_0 r^{\phi} \exp(-\psi r)$, with $\alpha_0 = 1.00 \pm 0.12$, $\phi = -0.05 \pm 0.02$, and $\psi = 5.78 \pm 4.79$. The $\chi^2$ value is given by 1.

## V. DISCUSSION

With some graphs in the $N$-$r$ plane, we can illustrate the finite-size behaviors of the ratio $R_K^2/R^2$ discussed in Sec. III. We recall that the topological effect has played a central role as well as the excluded-volume effect. Thus, we consider two lengths with respect to the number $N$ of polygonal nodes: the characteristic length of random knotting $N_c(r)$ and the ''excluded-volume length'' $N_{ex}(r)$. When $N > N_{ex}(r)$, the excluded-volume effect should be important to any $N$-noded SAP with radius $r$ .

We define $N_{ex}(r)$ by $N_{ex}(r) = 1/r^2$. The derivation is given in the following. We first note that the parameter $z$ of the excluded-volume is given by $z = \text{const} \times \sqrt{N} B/\ell^3 \propto N^{1/2} r$, where the cylindrical segments have the diameter $d$ and the length $\ell$, and the second virial coefficient $B$ of a polymer chain is given by $\ell^2 d$ [25]. Here we also note that the ratio $d/\ell$ corresponds to the radius $r$ of the cylindrical SAPs. We may consider that when $z \approx 1$, the excluded volume cannot be neglected. Thus we have the number $N_{ex}(r)$ from the condition $\sqrt{N_{ex}(r)}\, r = 1$.

We consider two graphical lines in the $N$-$r$ plane: $N = N_{ex}(r)$ and $N = N_c(r)$. In Fig. 7, the vertical line expresses the $r$ axis and the horizontal one the $N$ axis. The graph $N_c(r) = N$ reaches the $N$ axis at $N = N_c(0) \approx 300$. Here we recall that the function $N_c(r)$ is given by Eq. (2): $N_c(r) = N_c(0) \exp(\gamma r)$. There is a crossing point for the two curved lines. The coordinates of the crossing point are approximately given by $N^* = 1300$ and $r^* = 0.03$. For a given simulation of the ratio $R_K^2/R^2$ with a fixed radius $r$, we have a series of data points located on a straight line parallel to the $N$ axis.

Let us first consider the case of small values of $r$ such as $r = 0.003$ and $r = 0.01$. From the simulation of Sec. III, it is shown that the effective expansion due to the topological constraint is large. This is consistent with the following interpretation of the $N - r$ diagram: if we start from the region near the $r$ axis and move in the direction of the $N$ axis, then we cross the line $N = N_c(r)$ before reaching another one $\sqrt{N} r = 1$; thus, we expect that the excluded volume remains small when the topological effect becomes significant.

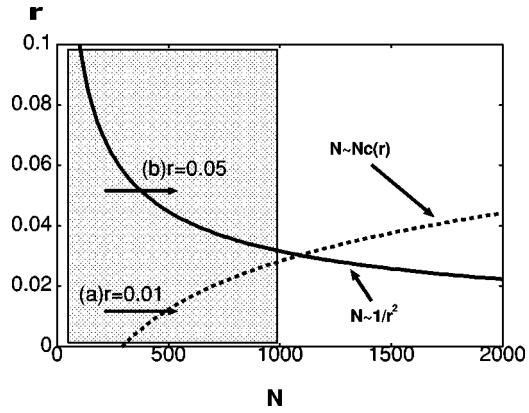


FIG. 7. $N$-$r$ diagram. Graphs of $N = N_c(r)$ and $N = N_{ex}(r)$ are shown by two curved lines. The arrows (a) and (b) suggest the series of the data points of Fig. 5 for $r = 0.01$ and $r = 0.005$, respectively. All the data points in the paper are located in the shaded area.

The above explanation should be consistent with the observation that the crossover of the trivial knot occurs near $N = N_c(r)$ for small values of $r$. Here we recall Figs. 3 and 4. When $r$ is very small, then we cross the line of $N_c(r) = N$ almost at $N_c(0) \approx 300$.

When radius $r$ is large such as $r = 0.03$ and 0.05, it is shown in Sec. III through simulation that the effective expansion is small: the ratio $R_K^2/R^2$ is close to 1.0. In the $N$-$r$ diagram, when we move rightwards from the region near the $r$ axis with $r$ fixed, we cross the line $\sqrt{N} r = 1$ before reaching another line $N_c(r) = N$. Thus, the effective expansion as the topological effect should be small.

Finally, we should remark that some important properties of $R_K^2$ of cylindrical SAPs with radius $r$ have been discussed systematically through scaling arguments with the blob picture by Grosberg [26]. In Ref. [26], the characteristic length $N_c(r)$ and the excluded-volume parameter $z$ are explicitly discussed in the $N$-$r$ diagrams. It would thus be an interesting future problem to investigate how far the predicted properties of $R_K^2$ are consistent with simulation results.

## ACKNOWLEDGMENTS

We would like to thank Professor K. Ito for helpful discussions. We would also like to thank Professor A. Yu. Grosberg for a helpful discussion and for sending the unpublished note on $R_K^2$ [26].

[1] A.V. Vologodskii, A.V. Lukashin, M.D. Frank-Kamenetskii, and V.V. Anshelevich, Zh. Eksp. Teor. Fiz. **66**, 2153 (1974) [Sov. Phys. JETP **39**, 1059 (1974)].
[2] J. des Cloizeaux and M.L. Mehta, J. Phys. (Paris) **40**, 665 (1979).
[3] M. Le Bret, Biopolymers **19**, 619 (1980).
[4] Y.D. Chen, J. Chem. Phys. **74**, 2034 (1981); **75**, 2447 (1981); **75**, 5160 (1981).
[5] J.P.J. Michels and F.W. Wiegel, Phys. Lett. A **90**, 381 (1982).
[6] K.V. Klenin, A.V. Vologodskii, V.V. Anshelevich, A.M. Dykhne, and M.D. Frank-Kamenetskii, J. Biomol. Struct. Dyn. **5**, 1173 (1988).
[7] E.J. Janse van Rensburg and S.G. Whittington, J. Phys. A **24**, 3935 (1991).
[8] K. Koniaris and M. Muthukumar, Phys. Rev. Lett. **66**, 2211 (1991).

[9] T. Deguchi and K. Tsurusaki, J. Knot Theory Ramif. **3**, 321 (1994).
[10] T. Deguchi and K. Tsurusaki, Phys. Rev. E **55**, 6245 (1997).
[11] E. Orlandini, M.C. Tesi, E.J. Janse van Rensburg, and S.G. Whittington, J. Phys. A **31**, 5953 (1998).
[12] Yu-Jane Sheng, Pik-Yin Lai, and Heng-Kwong Tsao, Phys. Rev. E **58**, R1222 (1998).
[13] M.K. Shimamura and T. Deguchi, Phys. Lett. A **274**, 184 (2000).
[14] M.K. Shimamura and T. Deguchi, J. Phys. Soc. Jpn. **70**, 1523 (2001).
[15] M.K. Shimamura and T. Deguchi, Phys. Rev. E **64**, R020801 (2001).
[16] J. des Cloizeaux, J. Phys. (France) Lett. **42**, L433 (1981).
[17] J.M. Deutsch, Phys. Rev. E **59**, R2539 (1999).
[18] A.Yu. Grosberg, Phys. Rev. Lett. **85**, 3858 (2000).
[19] V.V. Rybenkov, N.R. Cozzarelli, and A.V. Vologodskii, Proc. Natl. Acad. Sci. U.S.A. **90**, 5307 (1993).
[20] S.Y. Shaw and J.C. Wang, Science **260**, 533 (1993).
[21] T. Deguchi and K. Tsurusaki, Phys. Lett. A **174**, 29 (1993).
[22] M. Polyak and O. Viro, Int. Math. Res. Notices **11**, 445 (1994).
[23] M. K. Shimamura, Ph.D. thesis, Ochanomizu University, December 2000.
[24] M.K. Shimamura and T. Deguchi, J. Phys. A (to be published), e-print cond-mat/0108529.
[25] A.Yu. Grosberg and A.R. Khokhlov, *Statistical Physics of Macromolecules* (AIP Press, New York, 1994).
[26] A.Yu. Grosberg (private communication).